

**Key Points:**

- Micrometeorites are predicted to be far more abundant on Mars than on Earth
- Micrometeorites are concentrated in the residue of aeolian sediment removal, such as at bedrock cracks and gravel accumulations
- Micrometeorite accumulation sites are enriched in key nutrients for primitive microbes: reduced phosphorus, sulfur, and iron

**Correspondence to:**

A. G. Tomkins,  
andy.tomkins@monash.edu

**Citation:**

Tomkins, A. G., Genge, M. J., Tait, A. W., Alkemade, S. L., Langendam, A. D., Perry, P. P., & Wilson, S. A. (2019). High survivability of micrometeorites on Mars: Sites with enhanced availability of limiting nutrients. *Journal of Geophysical Research: Planets*, 124, 1802–1818. <https://doi.org/10.1029/2019JE006005>





Received 15 APR 2019

Accepted 17 JUN 2019

Accepted article online 27 JUN 2019

Published online 10 JUL 2019

## High Survivability of Micrometeorites on Mars: Sites With Enhanced Availability of Limiting Nutrients

Andrew G. Tomkins<sup>1</sup> , Matthew J. Genge<sup>2,3</sup> , Alastair W. Tait<sup>1,4</sup> , Sarah L. Alkemade<sup>1</sup>, Andrew D. Langendam<sup>1</sup>, Prudence P. Perry<sup>1</sup>, and Siobhan A. Wilson<sup>5</sup> 

<sup>1</sup>School of Earth, Atmosphere and Environment, Melbourne, Victoria, Australia, <sup>2</sup>Impact and Astromaterials Research Centre, Department of Earth Science and Engineering, Imperial College London, London, UK, <sup>3</sup>Department of Mineralogy, The Natural History Museum, London, UK, <sup>4</sup>Department of Biological and Environmental Sciences, University of Stirling, Scotland, UK, <sup>5</sup>Department of Earth and Atmospheric Sciences, University of Alberta, Edmonton, Alberta, Canada

**Abstract** NASA's strategy in exploring Mars has been to follow the water, because water is essential for life, and it has been found that there are many locations where there was once liquid water on the surface. Now perhaps, to narrow down the search for life on a barren basalt-dominated surface, there needs to be a refocusing to a strategy of “follow the nutrients.” Here we model the entry of metallic micrometeoroids through the Martian atmosphere, and investigate variations in micrometeorite abundance at an analogue site on the Nullarbor Plain in Australia, to determine where the common limiting nutrients available in these (e.g., P, S, Fe) become concentrated on the surface of Mars. We find that dense micrometeorites are abundant in a range of desert environments, becoming concentrated by aeolian processes into specific sites that would be easily investigated by a robotic rover. Our modeling suggests that micrometeorites are currently far more abundant on the surface of Mars than on Earth, and given the far greater abundance of water and warmer conditions on Earth and thus much more active weather system, this was likely true throughout the history of Mars. Because micrometeorites contain a variety of redox sensitive minerals including FeNi alloys, sulfide and phosphide minerals, and organic compounds, the sites where these become concentrated are far more nutrient rich, and thus more compatible with chemolithotrophic life than most of the Martian surface.

**Plain Language Summary** NASA's exploration program has allowed the scientific community to demonstrate clearly that Mars had a watery past, so the search for life needs to move on to identifying the places where water and nutrients coincided. We have investigated the relative abundance of micrometeorites on Mars compared to the Earth because these contain key nutrients that the earliest life forms on Earth used, and because their contained minerals can be used to investigate past atmospheric chemistry. We suggest that micrometeorites should be far more abundant on the Martian surface than on Earth's, and that wind-driven modification of sediments is expected to concentrate micrometeorites, and their contained nutrients, in gravel beds and cracks in exposed bedrock.

### 1. Introduction

The evolution of Mars' atmosphere is of interest because it controls the possibility of the initiation of life and its duration in a setting that may have at times been analogous to the early Earth. Currently, the atmosphere of Mars is too thin to support bodies of liquid water, or allow sufficient greenhouse warming to create temperate conditions suitable for life, on the surface. But there is good evidence that abundant water once flowed across the surface (Hynek, 2016), and thus, conditions have been more clement.

Recently, we demonstrated that fossil micrometeorites, preserved in ancient sedimentary rocks (2.7 Ga) on Earth, can be used to examine the chemistry of the upper atmosphere across geological time (Tomkins et al., 2016). This is possible because many micrometeorites melt and chemically equilibrate with a narrow band of the atmosphere (on Earth, 95–65-km altitude, depending on entry parameters and atmospheric density; cf. Rimmer et al., 2019) as they are heated during atmospheric entry. The most useful are a group known as I-type cosmic spherules (Genge et al., 2017); these are small particles of FeNi metal liberated from stony asteroids during collisions, which melt and become oxidized as they are slowed from cosmic velocities of several kilometers per second to terminal velocities on the order a few hundred kilometers per hour

(Genge, 2016), slowing with decreasing altitude. Thus, if I-type cosmic spherules can be found on the current surface, within sedimentary rocks on Mars, or within Martian meteorites, they can be used to investigate the chemistry of its atmosphere in the past.

Meteorites have already been found on Mars by the Opportunity, Spirit, and Curiosity rovers (Ashley et al., 2011; Schröder et al., 2008; Schröder et al., 2016). And, in situ analyses of the Martian regolith have been used to estimate that 1–3 wt % is composed of meteoritic material (Bland & Smith, 2000; Yen et al., 2006). Since the dominant majority of the total mass of solid material entering modern planetary atmospheres is cosmic dust in the submillimeter-size fraction (e.g., Folco & Cordier, 2015), most of this regolith-hosted meteoritic material is likely to have originated as cosmic dust. A broad variety of cosmic spherules, which form by melting of cosmic dust in Earth's atmosphere, has been described from micrometeorite collections obtained from Antarctica, deep-sea sediments, and deserts (Duprat et al., 2007; Folco & Cordier, 2015; Genge et al., 2008; Taylor et al., 1998). In addition to the I-type micrometeorites discussed here, cosmic spherule types include (1) glass, which are almost entirely silicate glass; (2) cryptocrystalline, containing crystallites of silicates and iron oxides; (3) barred olivine, consisting of mostly skeletal crystals of olivine in glass; (4) porphyritic, containing olivine microphenocrysts in glass; (5) G-type, containing approximately equal amounts of Fe oxide dendrites and silicate glass, often with metal and/or sulfide beads; (6) coarse-grained, containing >50% relict minerals; and (7) CAT, enriched in Ca, Al, and Ti with Mg/Si > 1.7, with barred olivine textures. Unmelted and partially melted micrometeorites have also been described, and some of these are extremely carbonaceous (Duprat et al., 2010; Folco & Cordier, 2015; Genge et al., 2008).

It has been suggested that stony meteorites on Mars, which may survive on the surface for billions of years, may be useful for investigating the past climate through examination of their weathering history (Schroder et al., 2016). Furthermore, it has been suggested that some of these may be useful to the detection of life on Mars (Tait et al., 2017), primarily because some meteorite groups have troilite (FeS) with well-constrained, low-variability  $\delta^{34}\text{S}$  signatures compared with the very large  $\delta^{34}\text{S}$  variability of Martian rocks. Sulfide minerals were (and still are) a key part of the life cycles of the earliest organisms on Earth (Brimblecombe, 2014; Nisbet & Fowler, 2014). Because sulfur-utilizing chemolithotrophs and heterotrophs strongly fractionate S isotopes, their presence can be recognized by atypical  $\delta^{34}\text{S}$  signatures in weathered meteorites (Tait, Wilson, et al., 2017), even when they are present at very low abundance in a microbial community (Tait et al., 2017). Some micrometeorites also contain sulfide minerals (detail below), and they are expected to be several orders of magnitude more abundant (by mass) on the Martian surface than stony meteorites, so they would be favorable sites for microbial Fe and S cycling, and an ideal target in the search for isotopic evidence of life.

Organisms on Earth are sometimes referred to as “CHNOPS” organisms owing to the very high (commonly >99 wt %) abundance of these elements in biomass (Morowitz, 1968). C, N, P, and S, as well as the trace nutrient Fe, are considered to be limiting nutrients: elements that limit biological growth (Kirkby et al., 2011). Meteorites and micrometeorites contain abundant Fe and S in reduced form. Phosphorus is also a common, albeit minor, component of the extraterrestrial flux to the planets (Pasek & Lauretta, 2008), occurring in reduced form in schreibersite ((Fe,Ni)<sub>3</sub>P) and/or oxidized form in apatite (Ca<sub>5</sub>(PO<sub>4</sub>)<sub>3</sub>F,Cl,OH), depending on the oxidation state of the source asteroid. And, carbonaceous micrometeorites contain biologically important molecules such as soluble organics, including amino acids (the building blocks of DNA, ribonucleic acid, and proteins; Brinton et al., 1998; Dartois et al., 2013). In comparison, bioavailable nitrate compounds are abundant in Martian soil and sedimentary rocks (Stern et al., 2015). Highly oxidizing (per) chlorates, which can be deleterious to life, are also abundant in Martian soil and sedimentary rocks (Stern et al., 2017), although microbes from evaporite environments on Earth have been found to survive equivalent environments (Al Soudi et al., 2017).

To investigate the possibility that micrometeorites are preserved on Mars, and their likely abundance and physical characteristics, we have modeled the entry of meteoritic dust through the current atmosphere. We have focused primarily on I-type spherules because (1) these are the best suited to investigations of past atmospheric oxidation state; (2) reduced phosphides and sulfides, which would be ideal for biological exploitation on the oxidized Martian surface, are associated with meteoritic iron (Pasek & Lauretta, 2008); and (3) these are more dense than other micrometeorite types and thus better suited to gravitational concentration by surface processes. An examination of aeolian transport of the resulting micrometeorites under current

Martian atmospheric conditions was then undertaken to investigate whether they are likely to be concentrated in favorable sites. And, to provide field-based support for this work, we investigated the variability in micrometeorite abundance at analog sites on the Nullarbor Plain in South Australia. The results imply that micrometeorites are abundant on the current Martian surface, and that they are likely to become concentrated at a variety of different sites by aeolian processes. Recognizing these sites allows targeting of material with greater potential to contain signs of life in the upcoming Mars2020 sample caching mission, prior to return of samples to Earth, and other missions.

## 2. Methods

### 2.1. Micrometeoroid Atmospheric Entry Model for Mars

We have generated a numerical model for the atmospheric entry of iron micrometeoroids at Mars to evaluate the probable size distribution and mineralogical nature of I-type cosmic spherules on the Martian surface. The model is based on that for the Earth (Genge, 2016), and includes evaporative mass loss and radiative cooling, following the methods of Love and Brownlee (1991). To model the formation of I-type micrometeorites within the Martian atmosphere, an improved treatment of oxidation was developed that incorporates reaction rates with Martian atmospheric CO<sub>2</sub>.

The calculations were conducted using a split scaling law, with a scale height of 11.7 km for altitudes below 30 km, and 7.9 km at greater altitudes (Flynn & McKay, 1990). Atmospheric composition for Mars was assumed constant up to altitudes of 100 km, and insignificant oxidation occurs at higher altitudes. A model of Earth's current atmosphere was used for comparison and is based on the 1976 Standard Atmosphere. The numerical model of entry heating makes two assumptions in treating deceleration and heating: (1) that gas flow is in the free molecular flow regime and (2) that particles are thermally homogeneous.

Free molecular flow occurs when the mean free path of atmospheric molecules exceeds the size of the micrometeoroid; consequently, incident molecules are unlikely to encounter reflected molecules, and thus collide directly with the particle's surface to cause heating. When the mean free path is significantly less than the size of the micrometeoroid, intermolecular collisions occur and a bow shock of compressed gas develops, allowing slip flow of gas over the surface of the particle. In the slip flow regime significant heating occurs owing to adiabatic compression of gas within the air cap, causing thermal radiation to the surface of the micrometeoroid. The mean free path of atmospheric gas at ~80 km on Mars is ~7.8 mm, and consequently, particles less than ~2,000- $\mu$ m diameter can be considered to be in the free molecular flow regime.

Thermal gradients within micrometeoroids have been shown to be of minor importance in particles up to 1 mm in diameter (Love & Brownlee, 1991). In larger particles, however, thermal gradients lead to enhanced surface temperatures relative to the interior and thus greater evaporative mass and radiative energy losses for a given amount of energy. Results for particles >1 mm, therefore, are likely to underestimate peak temperatures and result in slightly larger residual particles. This effect may be minimized once melting occurs, however, since vigorous mixing and heat transport is likely in the liquid state, which minimizes thermal gradients. Since the homogeneous compositions of terrestrial I-type spherules provide evidence that they crystallized from well-mixed liquids (Genge et al., 2017), the current simulations assume thermal homogeneity. The longer duration of heating during entry through the Martian atmosphere (see below) would tend to promote thermal homogeneity in larger particles than on Earth.

#### 2.1.1. Oxidation Model

The Martian atmosphere is dominated by CO<sub>2</sub> with an average of 95.32 wt %, and only traces of the other important redox gases O<sub>2</sub> (0.13 wt %) and CO (0.08 wt %; Owen et al., 1977). It has a relatively constant composition of the main gases up to altitudes of ~100 km (Chaffin et al., 2017). Consideration of FeNi metal oxidation in CO<sub>2</sub> is thus central to understanding the formation of I-type cosmic spherules on Mars. Experiments on oxidation of iron metal in CO<sub>2</sub>-CO gas mixtures reveal that the rate determining step is the interfacial reaction through the dissociative chemisorption of CO<sub>2</sub> to gaseous CO + adsorbed O (Li et al., 2000). In the experiments, surface blocking by an existing oxidized rind limits CO<sub>2</sub> dissociation, which then becomes dependent on the gas CO<sub>2</sub>/CO ratio, with CO removing a proportion of absorbed oxygen. The Martian atmosphere has a very large CO<sub>2</sub>/CO ratio up to altitudes of ~100 km, and an O<sub>2</sub>/CO ratio of 1.6, and reduction by CO can thus be ignored. The oxidation rates of iron in pure CO<sub>2</sub> determined by Li et al. (2000) are used in the current study where the reaction rate constant (in mol O m<sup>-2</sup> s<sup>-1</sup> atm<sup>-1</sup>) is

$$k = 34.43 \exp\left(-\frac{193,600}{RT(K)}\right) \quad (1)$$

Oxidation rates are, however, are dependent on partial pressure (Li et al., 2000).

The other oxidant in the Martian atmosphere is O<sub>2</sub>, which, although only present in trace abundances at 0.13 wt %, still has an impact on oxidation. Oxidation of liquid iron metal by oxygen occurs by adsorption of O<sub>2</sub>, charge transfer from Fe<sup>0</sup>, and dissociation of the O<sub>2</sub><sup>4-</sup> molecule (Radzilowski & Pehlke, 1978). Experimental studies suggest a two-stage behavior: (1) an initial stage where reaction rate is linear and lasting up to 30 s and (2) a later stage with lower parabolic reaction rates limited by the decreasing rate of oxygen diffusion across the thickening oxide layer. Reaction rates for the linear stage of oxidation, which applies to short-duration heating of atmospheric entry, are thought to be controlled by the kinetics of the surface reaction mechanism. Reaction rates for this stage have been determined by Abuluwefa et al. (1996) who gave a reaction rate constant (in kg O m<sup>-2</sup> s<sup>-1</sup>) of

$$k = 0.055 \exp\left(-\frac{17,000}{RT(K)}\right) \quad (2)$$

This expression is based on experiments in the temperature range 1,000–1,200 °C. Reaction rate, as for CO<sub>2</sub>, is dependent on the concentration of oxygen, here in kg/m<sup>3</sup>.

Pressure or gas density dependence can be explained by the dissociative chemisorption of O<sub>2</sub> or CO<sub>2</sub> as a function of the number of reactive sites available for chemical bonding to oxygen atoms that are physically absorbed on the surface. At low oxygen partial pressures and high temperatures, oxygen absorption on the surface is the rate-controlling step, assuming absorption equilibrium with the gas, and oxidation is thus temperature dependent. At very high oxygen partial pressures the availability of chemisorption sites is likely to be rate limiting and reaction rates become independent of gas partial pressure or density. However, during atmospheric entry the partial pressure at the micrometeoroid is dictated by the ram pressure, which is related to the atmospheric pressure  $\rho_a$  and particle velocity,  $v$ , by  $\rho_a v^2$ . Oxygen concentration can be calculated from ram pressure, assuming that the atmosphere behaves as an isothermal ideal gas; a reasonable assumption since no bow shock forms on such small particles.

Finally, oxidation is an exothermic process and consequently adds to the heating of particles. A value for the latent heat of iron oxidation to wüstite, of 3,785,660 J/g, is therefore included in the heat budget of the micrometeoroid. The oxide liquid shell generated by oxidation of metal is assumed to have the composition of stoichiometric wüstite (FeO). Once metal has been completely consumed by oxidation further oxygen is added to the oxide melt, leading to the formation of magnetite. A magnetite to wüstite ratio can then be calculated from the Fe and O abundance, assuming an assemblage in thermodynamic equilibrium. Studies of I-type spherules (Genge et al., 2017) suggest that this is broadly appropriate, although some additional magnetite formation may occur at low temperatures under nonequilibrium conditions.

### 2.1.2. Size Distributions

To predict the size distribution of I-type spherules on Mars a model for the initial size and velocity distribution in the Martian atmosphere is needed. The size distribution model for dust particles in the inner solar system by Grun et al. (1985) is used here, and is consistent with results from the Pioneer 8 and 9 missions, as well as measurements on the dust flux at the Earth's orbit from microcraters on the Long Duration Exposure Facility satellite (Love & Brownlee, 1993). A velocity distribution for micrometeoroids at Mars is derived from the distribution measured by Southworth and Sekanina (1973) in the Earth's atmosphere using the same approach as Flynn and McKay (1990) and Morgan and Zook (1988). This approximation incorporates the effects of gravitational focusing by Earth and Mars, and differences in semimajor axis. The postentry size distributions of several types of I-type particle were assessed including unmelted metal grains, metal-wüstite spherules, and wüstite-magnetite spherules. Results were obtained by binning the final diameters of particles after atmospheric entry heating. Results were normalized to the incident flux of interplanetary dust.

## 2.2. Concentration in Aeolian Traps

On Earth heavy minerals can be gravitationally concentrated in sedimentary traps owing to their high densities. Aeolian traps form when decreases in wind speed develop in the lee of obstacles, and the larger and

denser particles can no longer be transported. Winds can also remove smaller and less dense particles from aeolian sediments, leaving a residue enriched in larger and denser particles, in a process known as winnowing. Vertical fractures such as joints within bare rock surfaces are particularly efficient wind traps, and our analog site demonstrates (see below) that these do become enriched in micrometeorites through aeolian processes.

Aeolian concentration of heavy minerals with vertical fractures depends on two important factors: (1) the ability of grains to be transported laterally in the wind, so they can be delivered into the trap from a wide catchment area, and (2) the inability of the densest grains within the trap to be removed. Bagnold (1941) gave a simple expression for the threshold wind shear velocity that can transport grains by saltation as

$$u = A \sqrt{\frac{(\rho_p - \rho_a)}{\rho_a} g D} \quad (3)$$

where  $\rho_a$  and  $\rho_p$  are the atmospheric and particle densities, respectively;  $g$  is the gravitational acceleration; and  $D$  is the particle diameter. The constant  $A$  is a function of interparticle forces and Bagnold (1941) gave a value of 0.1 for loose sand. To calculate whether micrometeorites can move by saltation we used a Martian surface atmospheric density of  $0.02 \text{ kg/m}^3$  and  $g = 3.711 \text{ m/s}^2$ ; higher wind shear velocities are likely earlier in the history of Mars when atmospheric density was likely higher (cf. Catling & Kasting, 2017).

Evaluating the removal of particles from vertical fractures on bare rock surfaces can be achieved by considering the lift generated by the pressure drop associated with wind blowing across the surface. Balme and Hagermann (2006) discussed lifting of particles by dust devils on Mars by negative pressure excursions, which is analogous to the removal of grains from a vertical crack; they provide an expression for buoyancy of

$$F = \frac{3\Delta P}{2D\rho_p g} \quad (4)$$

where  $\Delta P$  is the pressure excursion, which Balme and Hagermann (2006) gave as a maximum of 5 Pa for Martian dust devils, and  $F$  is the ratio between lift and gravitational force, where values greater than 1.0 indicate lifting.

A similar analysis can be applied to winnowing of grains owing to the pressure excursion produced by a horizontal wind blowing over the surface, where  $\Delta P$  can be estimated by the Bernoulli principle as  $0.5 \rho_a v^2$ . Maximum wind speeds on Mars are estimated at 24 m/s (see Jackson et al., 2015), and these would generate  $\Delta P$  of 5.8 Pa, allowing estimation of the upper particle size limits, for grains with differing densities, that can be removed from a trap.

### 2.3. Micrometeorites From a Mars Analog Site

The conceptual basis for this field study comes from the recognition that wind-driven (or water-driven) sediment migration across a cracked bedrock surface leads to preferential accumulation of dense particles, including micrometeorites, in the cracks. Images of the Martian surface collected by both Opportunity and Curiosity clearly show that bedrock cracks have preferentially accumulated larger gravel particles and spherical hematite nodules (e.g., Figures 1a and 1b), indicating that aeolian processes have concentrated heavier particles in these cracks. Several other examples where aeolian processes have concentrated heavier particles have been found, including in the lee of positive topographic features (Figure 1c), and on sand dune tops where larger sand grains tend to be concentrated (Figure 1d).

We conducted field work on the Nullarbor Plain in South Australia, which we use as an analogue for the bedrock cracking and overlying sand dune migration observed by the Mars Science Laboratory Curiosity rover (Curiosity henceforth) in Gale Crater, and Mars Exploration Rover Opportunity (Opportunity henceforth) on Meridiani Planum, on Mars. It has previously been recognized that a combination of ice and aeolian transport promoted micrometeorite accumulation in joints in granite at the Transantarctic Mountains (Rochette et al., 2008), but this is quite a different setting to the deserts of Mars. The Nullarbor Plain is a semidesert site characterized by a flat pavement of rarely exposed limestone, overlain by a thin cover of partially vegetation-stabilized, wind-blown sand and residual gravel. Due to the flat landscape, most of the

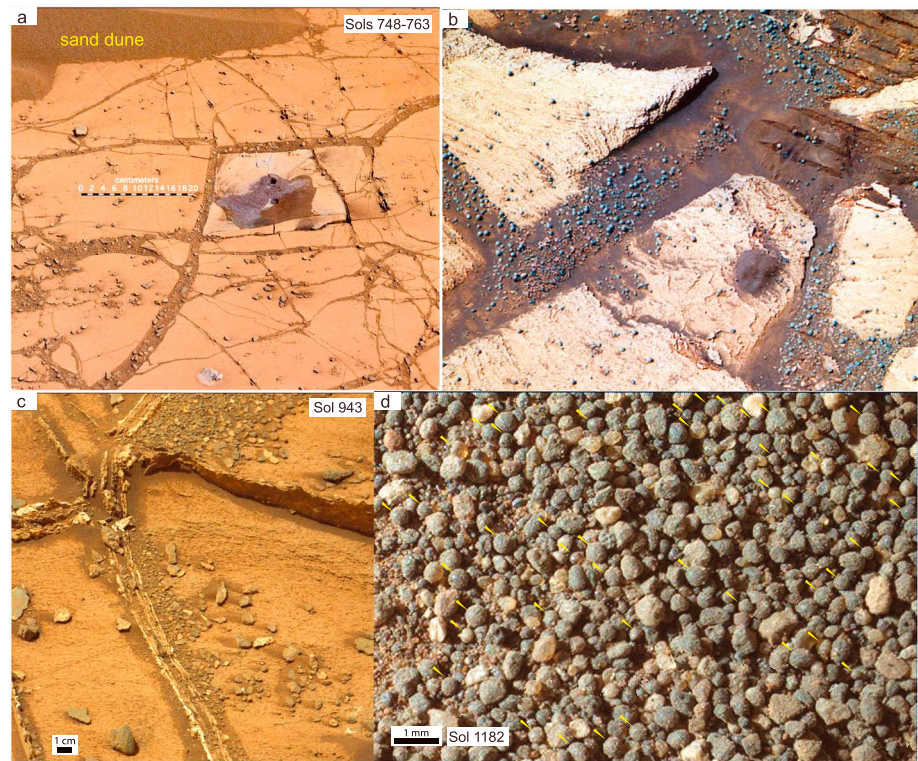


**Figure 1.** Examples of aeolian concentration of heavy particles on Mars. (a) Gravel particles in bedrock cracks imaged by Curiosity (right Mastcam) on sols 748–763. (b) A widely publicized image of spherical hematite concretions (“blueberries”) in bedrock cracks obtained by Opportunity (Pancam) on Meridiani Planum. (c) Gravel accumulated in the lee of erosion-resistant hydrothermal veins projecting from bedrock, imaged by Curiosity (right Mastcam) on sol 943. (d) Coarser sand particles (~200–900- $\mu\text{m}$  diameter) cementing the surface of a dune imaged by Curiosity (MAHLI) on sol 1182; yellow pointers indicate the position of highly spherical particles, some of which may be micrometeorites, based on our observed abundances on the Nullarbor Plain and the enhanced preservation on Mars.

overlying fine-grained sediment is wind-blown, although there are isolated sites where some short-distance waterborne migration has also occurred.

To examine variations in micrometeorite accumulation as a function of aeolian processes we collected sediment samples from several settings on the Nullarbor Plain: (1) within bedrock cracks (Figure 2a), (2) residual sand and gravel sitting immediately on flat bedrock (Figure 2b), (3) residual sand and gravel from the raised edge of clay-pans lacking bedrock (these are small ridges on the edge of depressions formed by wind erosion where heavier gravel particles are concentrated; Figure 2c), and (4) actively mobile, partially vegetation stabilized, meter-scale sand dunes (accumulated and frequently reprocessed by wind; Figure 2d).

In the lab, sediment samples were sieved into several size fractions (<38, 38–125, 125–250, 250–500, 500–2,000, >2,000  $\mu\text{m}$ ) using a stacked sieve set, which was cleaned using compressed air between each sample. Each size fraction greater than 250  $\mu\text{m}$  was then gravitationally sorted using a Wilfley table (sizes smaller than this are ineffectively sorted by this method). The denser fraction from this step was then magnetically subdivided (because most micrometeorites are magnetic) using an in-house magnetic sluice. Representative samples of the 125–250- $\mu\text{m}$  fraction from field each site were also magnetically subdivided without the gravitational separation step. The magnetic separates were then examined by optical microscopy and micrometeorites hand-picked based on their high degree of sphericity (melted micrometeorites are highly spherical). Unmelted micrometeorites tend to be porous, and partially melted micrometeorites tend to be scoriaceous, lowering their density, which means that most would not be gravitationally accumulated. Because the Nullarbor Plain is entirely composed of limestone there is very little dense magnetic material that is not extraterrestrial compared to most deserts (some material is blown in from deserts adjacent to the Nullarbor, but this consists mostly of quartz). Thus, we have a high degree of confidence that the dense, magnetic, highly spherical particles are cosmic spherules. Confirmation of the identity of a representative

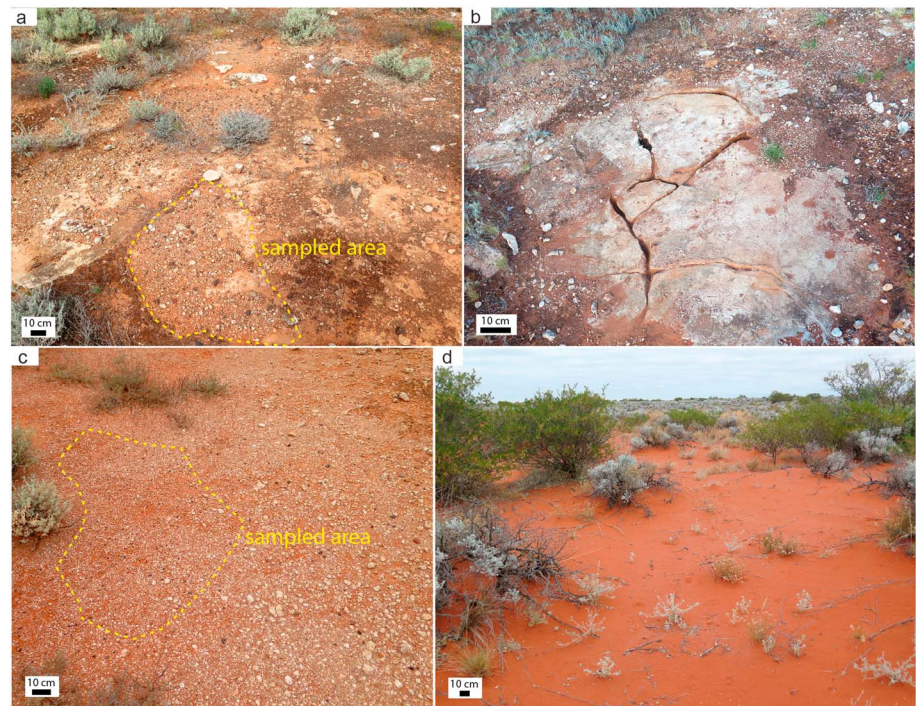


**Figure 2.** Examples of aeolian sorting from the analog field site on the Nullarbor Plain, which were sampled for micrometeorites. (a) Gravel on limestone bedrock, prior to sampling. (b) Cracks in limestone bedrock, exposed after excavation of the sample. (c) Gravel at the edge of a claypan, prior to sampling. (d) Wind-blown sand dunes, partially stabilized by vegetation. The sample was collected from approximately the top 2 cm of sand.

selection of micrometeorites was achieved by secondary electron imaging via scanning electron microscopy using a JEOL 7001F (field emission scanning electron microscopy), and all spherules were micrometeorites.

### 3. Results

#### 3.1. Micrometeorites From a Mars Analog Site

The results should be viewed in the context of the range of metal particle sizes in cosmic dust. Cosmic dust large enough to become cosmic spherules on Earth has been modeled to be derived from Jupiter family comets (~68%), collisions between inner solar system asteroids (~28%), and long period comets (5%); larger particles tend to come from the asteroids (Carrillo-Sánchez et al., 2016). Of these, only the inner solar system asteroids would contribute metal. Oxygen isotope data for 136 cosmic spherules support this model, with ~20% suggested to come from inner solar system asteroids (Cordier & Folco, 2014). Metal particle diameters average 300–500  $\mu\text{m}$  in unequilibrated chondrites (Dodd, 1976), and are typically <1 mm in achondrites, rarely exceeding 2 mm in meteorites in general (except in the comparatively rare CB chondrites, and iron and stony-iron meteorites).

Our simulations predict significantly lower peak temperatures (Figure 3) and thus enhanced survival of metallic micrometeoroids on Mars compared to the Earth, owing largely to lower entry velocities, but also lower atmospheric density. The minimum entry velocity for Mars is modeled to be 5.7 km/s, there is a peak in entry velocities at ~8 km/s, and ~90% of particles enter at <15 km/s (Figure 4). These parameters are close to recent estimates for much lower density silicate particles from asteroids and comets entering the Martian atmosphere (Borin et al., 2017). On Earth, evaporation limits the maximum size of micrometeorite spherules to about 2 mm diameter (cf. Rochette et al., 2008); however, on Mars spherules can theoretically reach several millimeters in diameter (Figure 5) since their relative mass loss is limited by the larger sizes required to reach sufficiently high temperature for melting. On Mars, the maximum I-type micrometeorite size is probably limited by the boiling temperatures of iron metal (3,134 K) and wüstite (3,687 K). At these temperatures the liquids lose mass rapidly through boiling with no further increase in temperature. Although no specific

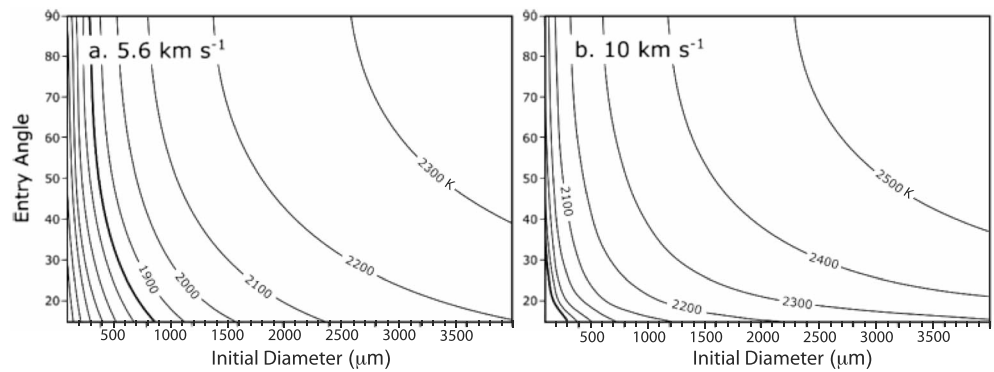


**Figure 3.** Peak temperatures experienced by iron micrometeoroids in the Martian atmosphere at different entry velocities (temperature contours in Kelvin; the bold line approximates the melting point of Fe), as a function of entry angle and initial diameter.

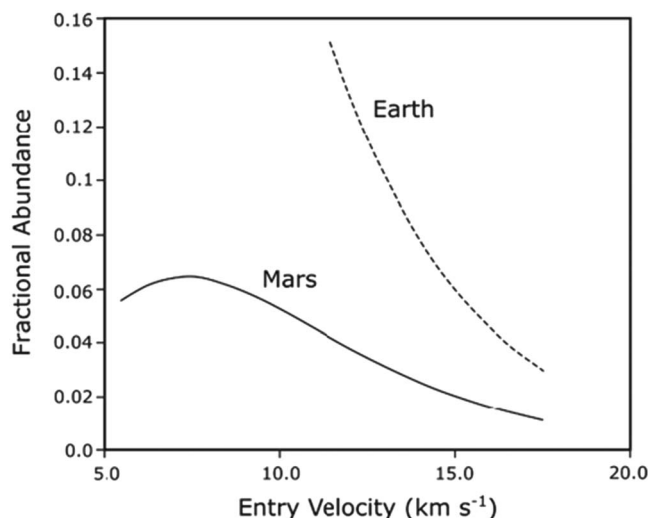
treatment of boiling was included in the current models, the boiling temperature of iron can be taken as a maximum limit to peak temperature and particle survival.

The results of calculations modeling the relative mass of iron metal remaining within I-type micrometeorites after oxidation by CO<sub>2</sub> during entry heating on Mars are shown in Figure 6. Very small amounts of iron oxide are generated during atmospheric entry owing to the competing low rate of CO<sub>2</sub>-associated oxidation and iron oxide loss through evaporation. The mass ratios of metal to oxide of 0.9994 to 0.9998 correspond to oxide layers just a few micrometers thick surrounding an FeNi metal core that formed as molten metal. This result indicates that Martian I-type micrometeorites are expected to be mineralogically very different to those on Earth, where complete oxidation of the metal is common (Genge et al., 2017), and evaporation is more extensive. It is clear that there is enhanced survival of reduced Fe and Ni on Mars, both of which are biologically useful (Ni is a micronutrient used in metalloenzymes on Earth). A further important mineralogical difference is that on Mars, the oxide liquid is predicted to crystallize only as wüstite, and these spherules will be composed of metal + wüstite with no magnetite present. Thus, the detection of ancient I-type cosmic spherules on Mars with thick wüstite shells, or particularly magnetite, would require a different atmospheric composition than today's, with greater oxidizing capacity at higher altitudes, such as increased O<sub>2</sub> or H<sub>2</sub>O.

The low degree of oxidation, combined with the lower temperatures, also has implications for the survival of biologically useful reduced P and S in schreibersite and troilite (FeS; although neither evaporation or oxidation of these was included in the primary models). These minerals are commonly associated with FeNi metal

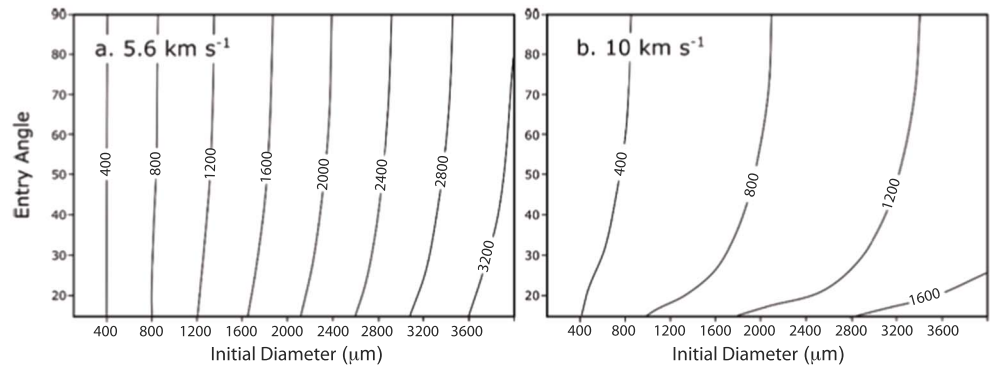
in a range of meteorite types (schreibersite is found in iron and stony-iron meteorites, reduced stony meteorites, and primitive chondrites), but incongruently decompose to metal + P or S gas at much lower temperatures than Fe evaporation (the rate increasing exponentially as a function of temperature; Tachibana & Tsuchiyama, 1998; Viksman & Gordienko, 1992). Based on Figure 3 and published data on mineral evaporation rates (Tachibana & Tsuchiyama, 1998; Viksman & Gordienko, 1992), we suggest that troilite in I-type micrometeorites would rarely survive atmospheric entry on Mars, whereas schreibersite would survive with little evaporation. The cooler temperatures and weak oxidation mean that schreibersite should be considerably more abundant in micrometeorites on Mars than on Earth. Despite the hotter temperatures and greater oxidation as a function of size experienced by micrometeorites at Earth, sulfide minerals and schreibersite are observed in rare micrometeorites (Khisina et al., 2016), indicating that they must occur on Mars.

Figure 7 shows that small unmelted unoxidized iron micrometeorites (< ~200- $\mu$ m diameter) are expected to represent the dominant proportion of the total I-type population on Mars, and these would be dominated by particles that had low entry angles and velocities; few larger unmelted



**Figure 4.** Initial velocity distributions for micrometeoroids encountering Earth and Mars.





**Figure 5.** Final diameters of I-type micrometeorites (contours) after evaporation in the Martian atmosphere, as a function of entry angle and initial diameter.

iron micrometeorites are expected. This lack of melting is important because it means that schreibersite and troilite would more commonly survive atmospheric entry and are thus expected to be present in some of the unmelted micrometeorites. All spherules become less abundant with increasing initial size, but the ratio of partially melted and oxidized to unmelted spherules increases greatly with increasing size due to the higher temperatures reached (Figures 3 and 7); the sharp dropoff in the number of particles above 3200- $\mu\text{m}$  diameter is due to evaporation.

The textures of Martian I-type micrometeorites can also be predicted by comparisons with terrestrial examples. Terrestrial I-types are typified by dendritic wüstite crystals enclosing smooth metallic beads (e.g., Tomkins et al., 2016, Figure 1), although the external features can be removed by abrasion in aeolian systems (Figures 8a and 8a). Decreases in cooling rate have been suggested to result in increases in crystal size, with the lowest cooling rates producing equant wüstite crystals (Genge et al., 2017). Our results indicate that the duration of heating experienced by Martian I-types is  $\sim 3$  times longer than that of terrestrial micrometeoroids, resulting in slower cooling rates (Figure 9). However, as Martian I-types are predicted to develop very thin wüstite shells, their exteriors are likely to be texturally different to terrestrial examples; probably with more equant wüstite crystals, consistent with slower cooling, confined to a thin exterior layer.

The current flux of I-type spherules to the Martian surface can be estimated if we assume that the abundance of metallic to silicate dust in the interplanetary population is the same at Mars as at Earth. Studies of terrestrial micrometeorites suggest an abundance of  $\sim 2\%$  I-types (Taylor et al., 2000). The flux of micrometeoroids to the Martian atmosphere has been estimated to be  $29,600 \pm 2,300$  t/year, which is  $\sim 0.53$  times that of Earth

at  $56,000 \pm 9,600$  t/year (Borin et al., 2017). Therefore, there is likely to currently be  $\sim 600$  t/year of FeNi metal dust entering the Martian atmosphere each year. It is difficult to accurately calculate how much S and P this would equate to because of the large differences in extent of heating and oxidation. If there was no evaporative mass loss there would be  $\sim 204.4$  g of micrometeorites per  $\text{km}^2$  accumulating on Mars every year, or  $2\%$  of the total is  $\sim 4$  g  $\text{km}^{-2} \text{yr}^{-1}$  I-types; a single 100- $\mu\text{m}$ -diameter metal-dominated I-type micrometeorite weighs  $4.1 \times 10^{-6}$  g, so this is equivalent in mass to about one 100- $\mu\text{m}$ -diameter I-type micrometeorite per  $\text{m}^2$  per year (or eight 50  $\mu\text{m}$  I-types  $\text{m}^{-2} \text{yr}^{-1}$ ; for further context, the abundance of micrometeorites increases exponentially with decreasing size; Taylor et al., 2000). On Earth the figure would be  $109.7$  g  $\text{km}^{-2} \text{yr}^{-1}$  for all micrometeorite types assuming no evaporative mass loss (the surface area of Mars is 28.4% that of Earth). The simulations here suggest only minor mass loss by evaporation, and enhanced survival of I-type micrometeorites at Mars compared to Earth; mass loss is known to be significant in Earth's atmosphere (Carrillo-Sánchez et al., 2015). Due to their greater density, metal particles take longer to decelerate in the atmosphere and thus experience greater heating than the silicate and carbonaceous

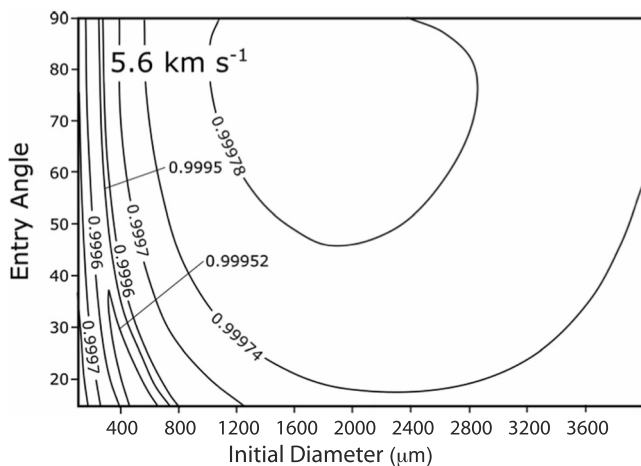


**Figure 6.** Mass of metal relative to wüstite within Martian micrometeorites at an entry velocity of 5.6 km/s (1.0 = 100% metal), as a function of entry angle and initial diameter.

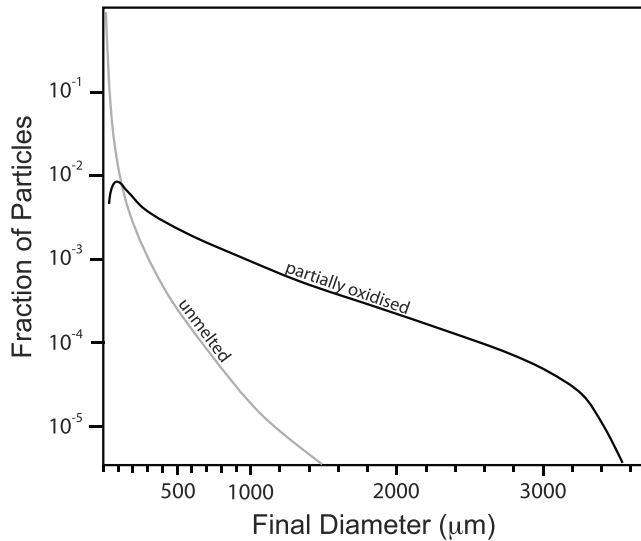


**Figure 7.** The size distribution of partially oxidized spherules (black) and unmelted metallic particles (grey) against final diameters normalized to the total initial flux.

micrometeorites. Therefore, the other micrometeorite varieties would also survive atmospheric entry better at Mars than Earth. During the Amazonian, the impactor flux is expected to have been a relatively constant low rate compared to the Noachian (cf. Hartmann, 2005; Quantin-Nataf et al., 2019), so the micrometeorite accumulation rate is not expected to have changed significantly in the last 3 billion years. Given these factors, and the extended age of the Martian surface owing to its low erosion rate and lack of water, far greater accumulation of micrometeorites is expected on Mars relative to Earth, particularly when a concentration mechanism such as aeolian gravitational sorting is also active (see more below).

### 3.2. Model for Modern Aeolian Concentration of Micrometeorites on Mars

Given recent estimates of wind shear speeds of 24.3 m/s in exposed areas on Mars (Jackson et al., 2015), our calculations suggest that I-type spherules up to several millimeters in size can be transported by saltation. Furthermore, I-type spherules  $>253 \mu\text{m}$  in diameter could not be winnowed by dust devils on Mars, while plagioclase must be  $>750 \mu\text{m}$  and olivine  $>610 \mu\text{m}$  to be retained in wind traps. We also estimate that winnowing by strong Martian winds can remove grains from a trap of up to 340, 710, and  $870 \mu\text{m}$  in diameter for I-types, olivine, and plagioclase (from erosion of basalts), respectively. Although this analysis is simple, it demonstrates that under current Martian atmospheric pressures and wind speeds, aeolian concentration of I-type micrometeorites is likely to occur within wind traps. Given that Martian surface has been dry since the early Amazonian, the atmospheric pressure is unlikely

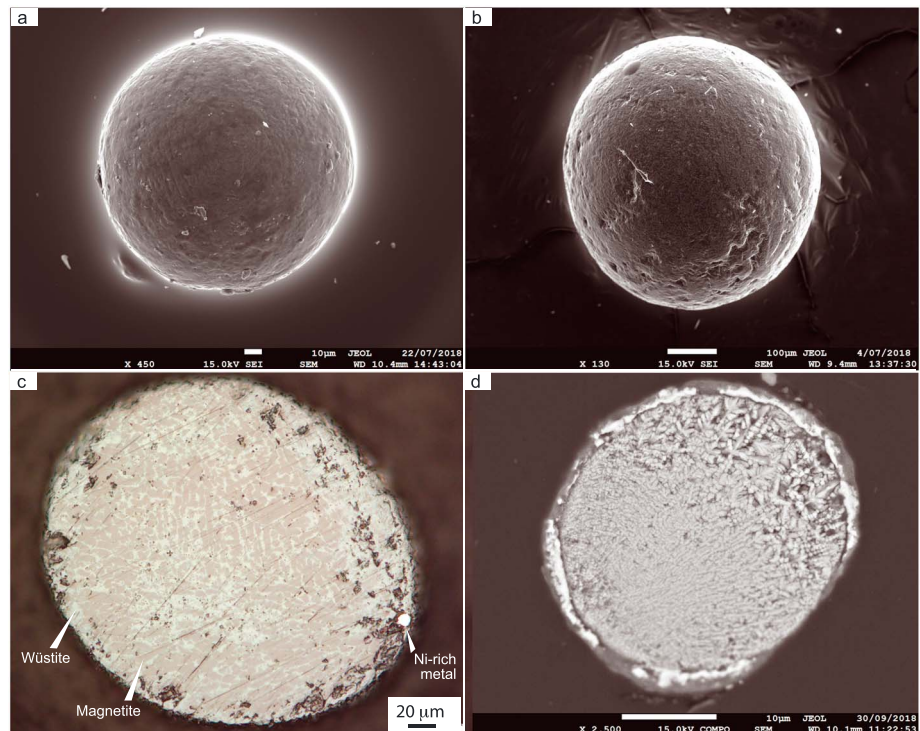


**Figure 8.** Examples of terrestrial micrometeorites from the Nullarbor Plain. (a and b) Examples of the exterior appearance of cosmic spherules affected by wind transport (secondary electron image). (c) Example of a sectioned I-type micrometeorite, showing denritic intergrowths of magnetite (reddish) and wüstite (light grey) and a small Ni-rich metal bead (reflected light). (d) Example of a sectioned cryptocrystalline cosmic spherule dominated by dendritic olivine crystals, the bright shell consists of iron oxides (BSE image).

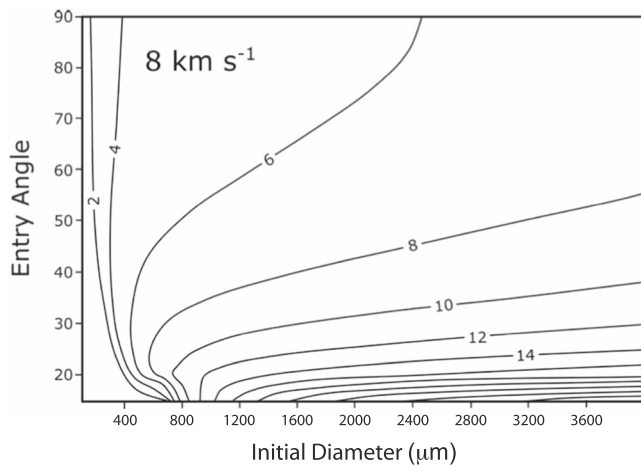


**Figure 9.** Time above the solidus for Martian I-type micrometeoroids in seconds, as a function of entry angle and initial diameter, entering at 8 km/s.

to have been significantly higher than the present during this period, so wind erosion is likely to have been comparable to today throughout the last 3 billion years; atmospheric pressure may have approached 1 bar during wet periods in the Hesperian (cf. Catling & Kasting, 2017).

### 3.3. Micrometeorite Accumulation at a Mars Analog Site

Numerous micrometeorites (over 1,600 in total, ranging in size from 17- to 523- $\mu\text{m}$  diameter; e.g., Figure 8) were collected from the sampled aeolian sediment accumulation sites on the Nullarbor Plain. We found the greatest abundance within bedrock cracks, and in residual gravel on bedrock; distinctly lower abundances were found on sand dune tops (Table 1). An important difference between the bedrock cracks on the Nullarbor Plain and those on Mars is that the former contain plant matter, including roots that stabilize the soil, making it less susceptible to aeolian reprocessing.

This enhanced micrometeorite abundance at sites where lighter material is removed by wind to leave residual gravel has occurred despite that fact that the micrometeorites are very small. This is likely to be due to their higher densities. Dense I-type micrometeorites can be distinguished from

other types based on their high magnetic susceptibility and reflectivity, and their relative abundance in the Nullarbor collection appears to be on the order of 60%. This relative abundance is far higher than the 2% I-type abundance seen in the Antarctic collections (Taylor et al., 2000; which are not affected by wind-based concentration mechanisms), consistent with density-based concentration enhancement.

## 4. Discussion

### 4.1. On the Location of Modern Micrometeorites on Mars

We suggest that micrometeorites have already been imaged on the Martian surface by Curiosity (e.g., perhaps Figure 1d), and probably Opportunity and Spirit, because they are expected to be far more abundant

**Table 1**  
Micrometeorite Abundance as a Function of Aeolian Setting on the Nullarbor Plain

Sample	Description	#MMs sorted from		Abundance (MM/kg)
		125–250- $\mu\text{m}$ sieved fraction	Weight sorted (g)	
Null-06	Gravel on limestone pavement	217	50	4340
Null-01b <sup>a</sup>	Gravel on limestone pavement	72	198	364
Null-12	Crack in limestone pavement	30	25	1200
Null-01a <sup>a</sup>	Crack in limestone pavement	40	69	583
Null-03	Residual gravel on claypan margin	144	564	255
Null-01c <sup>a</sup>	Biological soil crust	48	158	304
Null-10	Sand dune	11	50	220
Sample	Description	#MMs sorted from		Abundance
		250–500- $\mu\text{m}$ sieved fraction	Weight sorted (g)	
Null-06	Gravel on limestone pavement	91	197	462
Null-01b <sup>a</sup>	Gravel on limestone pavement	84	291	289
Null-12	Crack in limestone pavement	214	1433	149
Null-01a <sup>a</sup>	Crack in limestone pavement	12	47	257
Null-03	Residual gravel on claypan margin	301	1923	157
Null-01c <sup>a</sup>	Biological soil crust	6	105	57
Null-10	Sand dune	290	6863	42

<sup>a</sup>Null-01a–c were taken at the same location, from different settings. Biological soil crust is a friable 0.5–1-cm-thick crust of soil cemented by dried cyanobacteria, fungi, lichens, bryophytes, and algae; it is resistant to wind erosion and periodically develops shallow fractures through desiccation. The residual gravel found on the margins of claypans develops through wind-blown buildup of sand and gravel into low ridges, which are then eroded by wind to preferentially leave the heavier gravel particles.

there than on Earth. In 6.95 kg of sand from the surface of a typical dune on the Nullarbor Plain we found 275 micrometeorites; this was the lowest abundance of the various sites sampled. Although these sand dunes are small and young, they are derived from aeolian processing of a surface that has yielded meteorites that fell up to 35,000 years ago (Bevan et al., 1998). By comparison, very little geological change has happened in most places on Mars during the Amazonian, since deposition of the northern plains sediments, perhaps ~3 billion years ago (with considerable uncertainty on this age (cf. Tanaka & Hartmann, 2012), the poles and areas of Amazonian volcanism being the main exceptions). The age of the surface in Gale Crater currently being explored by Curiosity has been estimated at  $78 \pm 30$  Ma, exposed by wind erosion (Farley et al., 2014). Furthermore, the lack of standing surface water in that time frame, the comparatively mild wind strength, and lack of oxygen in the atmosphere, means that micrometeorite preservation potential during the Amazonian period is expected to be far higher on Mars than on Earth (many micrometeorites recovered from the Nullarbor are broken, caused by wind transport and rusting of the residual metal bead, which weakens their structure). However, chlorates and perchlorates ((per)chlorates) are moderately abundant (hundreds to thousands of milligrams per kilogram) in Martian soils and sedimentary rocks of Hesperian age and younger (Stern et al., 2017), and are known oxidizing agents that could potentially destroy or alter micrometeorites rich in reduced minerals. However, these nitrate and perchlorate concentrations are comparable to those found in surficial and vadose zones of desert soils on Earth (Lybrand et al., 2013), which are among the best places for preservation of meteorites. Based on oxidative weathering of iron in stony meteorites found by Opportunity, Schroder et al. (2016) found that the average long-term chemical weathering rates are 1–4 orders of magnitude slower than the slowest rates on Earth.

Experiments have shown that when chlorates and perchlorates are dissolved in chloride- or sulfate-bearing aqueous fluids, only chlorates cause oxidation of  $\text{Fe}^{2+}$  under Mars surface conditions and acidic to neutral pH (i.e., perchlorates do not; Mitra & Catalano, 2017). Although the surface of Mars is currently dry, (per)chlorates are strongly deliquescent, and (per)chlorate brines have very low freezing points, in some cases below  $-70$  °C (Al Soudi et al., 2017). There are thus likely to have been climatically suitable periods in relatively recent Martian history, particularly at higher latitudes where water was likely more mobile during high obliquity (Forget et al., 2006), when the (per)chlorates could extract enough water from the atmosphere to be more active as oxidizing agents. Despite this, the slow weathering rate of meteorites found on Mars (Schröder et al., 2016) indicates that micrometeorites would avoid oxidation on Mars far longer than on Earth.

The Martian aeolian traps shown in Figure 1 are places where elevated abundances of dense micrometeorites are expected to have accumulated after migrating short distances. In addition to the I-type micrometeorites modeled above, silicate-rich micrometeorites that contain FeNi metal, troilite, schreibersite, chromite, and/or magnetite are denser than typical Martian sand (which is dominated by olivine, pyroxene, and plagioclase; Bish et al., 2013), and therefore also accumulate in aeolian traps, albeit in lower abundances. Dense micrometeorites would also accumulate on residual surfaces in areas of deflation, where wind has removed small, light particles leaving larger and denser particles behind. Commonly on Mars, these deflation surfaces consist of gravel with minimal sand, gravel on bedrock, or bare bedrock, often as interdune regions. As dunes migrate, larger rock fragments, and likely dense micrometeorites, are stranded as a residual basal layer that builds over time. The surfaces of the windward side of dunes are also residual surfaces, but are much shorter-lived than the residual basal layer.

Images from the Opportunity and Curiosity rovers clearly show that blueberries (spherical hematite concretions) accumulate on hard stranding surfaces, and particularly in cracks on those surfaces (Figure 1b), as lighter sand and dust is removed by wind, and the host-rock eroded. Given that many micrometeorites are predicted to be of comparable size to the blueberries, or smaller, and be considerably denser due to retention of FeNi metal, they should be preferentially accumulated at the same sites. Indeed, Curiosity rover images of the residual surfaces of sand dunes show possible cosmic spherules, based on high degree of sphericity (shown in Figure 1d). The sampling conducted at our Nullarbor analog site tested some of these types of residual surfaces and aeolian traps and found enrichment in micrometeorites, by an order of magnitude in some cases, compared to active dune surfaces (Table 1).

Some micrometeorites on Earth lack dense minerals, and are dominated by olivine and glass, which are of comparable density to Martian sand, and therefore would not undergo any density-based aeolian

concentration. Scoriaceous and carbonaceous micrometeorites are less dense than typical Martian sand. These low-density micrometeorites may also become concentrated by aeolian processes, but in the opposite sense to the dense micrometeorites. These will tend to become airborne more easily than equivalent sized sand/dust particles, and so will tend to be found where the finest wind-blown dust preferentially accumulates. However, since fine dust is highly abundant on the Martian surface (Mangold et al., 2009), the low-density micrometeorites are unlikely to have become as concentrated by aeolian processes as the high-density micrometeorites.

#### 4.2. Fossil Micrometeorites on Mars

On Earth, fossil micrometeorites have been found in limestones and cherts (Onoue et al., 2011; Suttle & Genge, 2017; Tomkins et al., 2016), which have enhanced abundances relative to other sedimentary rocks due to their slow sediment accumulation rates. Although in some cases these fossil micrometeorites have been altered during diagenesis (Suttle & Genge, 2017), some of the oldest (2.7 Ga) retain the wüstite + FeNi metal that resulted from atmospheric entry (Tomkins et al., 2016). If they can survive the geologic rigors of the much more oxidized, hydrated, and tectonically active Earth system, micrometeorites are expected to be able to survive in some Martian sedimentary rocks. The question then becomes: which rocks?

We have identified several settings where dense micrometeorites could be concentrated within an exposed stratigraphic sequence on Mars: (1) at the base of aeolian dune sequences, (2) at heavy mineral or gravel enriched layers that formed as a result of winnowing, and (3) within desiccation cracks and other cracks developed in hard surfaces and then buried.

Wind erosion of sedimentary rocks containing micrometeorites will tend to conserve and concentrate the hard micrometeorites (wüstite has the same hardness as hematite) in the same way that blueberries have been liberated and concentrated at Meridiani Planum and Gale Crater. If micrometeorite-rich stranding surfaces and cracks are buried by later sedimentation or impact ejecta, and then lithified, they should be preserved as distinctive horizons that would be easy to investigate by rover.

Desiccation cracks, formed by drying out of muddy and clay-rich sediment layers in lakes, have the potential to be long-lasting exposed features in some places on Mars. As demonstrated above, the longer these cracks persist on the surface, the greater the accumulation of micrometeorites is. Burial through further sedimentation would then preserve micrometeorites preferentially within the cracks. Curiosity has found fossilized desiccation cracks (Stein et al., 2018), indicating that they are abundant enough on Mars to be a viable sampling target for current or future rovers. However, given that we found moderately abundant micrometeorites on the most recently transported sand dunes on the Nullarbor (220 micrometeorites/kg in the 125–250- $\mu\text{m}$  sieve fraction), and given the better preservation potential of the Martian surface, we expect that they would be more abundant in coarse fractions of aeolian sedimentary rocks on Mars.

#### 4.3. The Effect of Changes in Atmospheric Density and Chemistry on Micrometeorites

Fossilized I-type micrometeorites can be used to gauge past atmospheric chemistry because the wüstite: FeNi metal ratio will increase as a function of  $\text{O}_2$  abundance (Tomkins et al., 2016), and they provide an unfractionated record of the O isotope signature (Pack et al., 2017). In Earth's current atmosphere, there is sufficient  $\text{O}_2$  to completely consume the metal and start converting to the wüstite to magnetite in micrometeoroids that experienced longer heating periods (Genge et al., 2017); many retain FeNi metal. Observation of abundant wüstite in fossilized Martian micrometeorites would indicate a more oxidizing past atmosphere than is currently found. Similarly, observation of magnetite, if not produced by later surface pseudomorphic replacement of wüstite (which can be distinguished geochemically; Suttle & Genge, 2017), would indicate a far more oxidizing past atmosphere.

Higher abundances of water at the surface of Mars require greater atmospheric concentrations as well. Increased  $\text{H}_2\text{O}$  in the atmosphere would lead to more extensive UV-induced dissociation to  $\text{H}_2$ ,  $\text{O}_2$ ,  $\text{H}_2\text{O}_2$ , and several short-lived molecules (cf. Catling & Kasting, 2017). Since H preferentially escapes the atmosphere due to its low atomic mass, this leads to higher concentrations of  $\text{O}_2$  and  $\text{H}_2\text{O}_2$  in the atmosphere. This process is likely how Mars' relatively oxidizing atmosphere evolved, which led to production of the

iron oxide minerals that make its surface red and other oxidized minerals and compounds such as sulfates, nitrates, and (per)chlorates (Catling & Kasting, 2017). Although it is difficult to gauge what the atmospheric abundance of oxygen may have been in the past, sulfate- and iron oxide-rich sedimentary rocks are Late Noachian to Hesperian in age (Carr & Head, 2010; Hynek & Phillips, 2008), implying that much of the oxidation of the Martian surface occurred during this period. If so, micrometeoroids that fell at this time are likely to have been more extensively oxidized and so would have a greater chance of preservation, since wüstite and magnetite are more resistant to postdepositional chemical modification in an oxidizing environment than FeNi metal.

During the late Noachian, and to a lesser extent the early Hesperian, Mars likely had a sufficiently dense atmosphere to allow water to periodically persist at the surface and precipitate as rain and/or snow (Carr & Head, 2015; Wordsworth, 2016). Increased atmospheric density has the effect of increasing the deceleration rate of micrometeoroids, which leads to greater heating for each particle, and thus, fewer large particles would survive atmospheric entry. However, to approach the conditions that micrometeoroids experience at Earth, Martian atmospheric density would need to be considerably higher because of its lower gravity. Recent results from the MAVEN spacecraft suggest that the early atmosphere of Mars may have been comparable to Earth's current atmospheric density (Jakosky et al., 2017), with measured extensive losses of Ar requiring that most of the atmosphere has been lost to solar wind sputtering. Thus, ancient micrometeorites on Mars are likely to have always been bigger than those on Earth (due to its lower gravity).

#### 4.4. Significance for Putative Martian Biology

The earliest life forms on Earth are thought to have included chemolithotrophs (Weiss et al., 2016), which gain energy from oxidation of reduced minerals. I-type micrometeorites represent localized occurrences of extreme redox gradient on the Martian surface (i.e.,  $\text{Fe}^0$  in contrast to abundant  $\text{Fe}^{3+}$ ); their relatively reduced nature would make them energetically attractive targets to iron oxidizing chemolithotrophs if they ever existed there. On Earth, microorganisms that oxidize reduced transition metals and sulfur play an important role in mobilizing these nutrients, making the resulting oxidized compounds accessible to organisms that reduce sulfur- and redox-sensitive metals. We have suggested that the larger, minimally oxidized I-type micrometeorites expected on Mars may also occasionally contain reduced sulfur in the form of troilite and/or phosphorus in the form of schreibersite (other types of cosmic spherules would also contain these minerals). These minerals are energetically beneficial to chemolithotrophs because their oxidation involves large valence changes and thus greater energy production; the S can be oxidized from  $\text{S}^{2-}$  to  $\text{S}^{6+}$  in sulfates, the P can be oxidized from  $\sim\text{P}^-$  (see Pasek et al., 2015) to  $\text{P}^{5+}$  in phosphates, and the Fe can be oxidized to  $\text{Fe}^{3+}$  from  $\text{Fe}^{2+}$  and  $\sim\text{Fe}^{0.33+}$ , respectively.

The tendency of dense micrometeorites to preferentially accumulate in the aeolian traps identified above means that these will be localized niches that are more attractive to chemolithotrophs than most of the Martian surface. These are thus ideal targets for exploring for past or present life on Mars.

But perhaps more importantly, P is a key element for life and meteoritic schreibersite—the only source of reduced P on the Martian surface—has been implicated in the emergence of life on Earth through its ability to phosphorylate simple hydroxyl compounds to form the precursors for life (Gull et al., 2015). Complex organic compounds are abundant in carbonaceous meteorites and micrometeorites, although schreibersite is not known to occur in carbonaceous micrometeorites. However, FeNi metal and other dense phases do exist in some carbonaceous meteorites, and thus, some carbonaceous micrometeorites may be dense enough to accumulate in the same aeolian traps (also hydraulic traps) as schreibersite-bearing micrometeorites. These sites, when drowned in water, would be ideal for developing phosphorylated biomolecules (cf. Gull et al., 2015), potentially leading to the emergence of life. In this way, Mars may be an analog for the early Earth; by investigating the Martian surface we may be looking at clues to how life started on Earth. Furthermore, much of the Martian surface is covered in impact ejecta, some of which likely buried aeolian sediments, thereby creating pockets of habitability within the shallow subsurface of Mars, where water, organic compounds, and inorganic energy sources can coexist in a radiation-shielded and thermally stable environment. A currently active example may be preserved today under the polar ice caps (Orosei et al., 2018).

## 5. Conclusions

Our modeling implies that I-type micrometeorites should be abundant on the Martian surface, particularly at locations where aeolian sorting promotes accumulation of heavy particles. Such locations include bedrock cracks, residual gravel accumulations (particularly on bedrock), in the lee of wind-blocking objects, and in coarse sand layers formed by winnowing. Other dense micrometeorites containing FeNi metal, chromite, magnetite, or schreibersite should also be concentrated in the same settings. Fossil micrometeorites would be found in sedimentary sequences that preserve these settings, the most common of which are likely to be residual gravel or coarse sand accumulations within aeolian dune sequences. We further suggest that micrometeorites provide a better source of bioavailable limiting nutrients for life than the typical basaltic surface of Mars. And furthermore, settings where phosphide-bearing and organic compound-bearing micrometeorites have accumulated together in elevated abundances, which then become water-saturated, would produce the ideal physical and chemical conditions for the emergence of life.

## Author Contributions

A.G.T. conceived of and planned the project, conducted the field work, and wrote the paper. M.J.G. performed the atmospheric entry calculations and wrote the associated sections of the paper. A.W.T. conducted the field and lab work. S.L.A., A.D.L., and P.V.P. spent many hours in the lab separating micrometeorites. S.A.W. assisted with the discussion on Martian astrobiology.

## Acknowledgments

We thank Junnel Alegado for his assistance in technical support and sample preparation. Jennifer Mitchell is thanked for her contribution to scientific discussions relating to this project. This project was funded under Australian Research Council grants DP170101250 to A.G.T. and M.J.G. and DE150100770 to S.A.W. Micrometeorite and model data can be obtained from FigShare at doi:10.26180/5cb40283a798f and 10.26180/5d01733e6c79b.

## References

- Abuluwefa, H., Guthrie, R. I. L., & Ajersch, F. (1996). The effect of oxygen concentration on the oxidation of low-carbon steel in the temperature range 1000 to 1250 °C. *Oxidation Metals*, 46(5-6), 423–440. <https://doi.org/10.1007/BF01048639>
- Al Soudi, A. F., Farhat, O., Chen, F., Clark, B. C., & Schneegurt, M. A. (2017). Bacterial growth tolerance to concentrations of chlorate and perchlorate salts relevant to Mars. *International Journal of Astrobiology*, 16(3), 229–235. <https://doi.org/10.1017/S1473550416000434>
- Ashley, J. W., Golombek, M. P., Christensen, P. R., Squyres, S. W., McCoy, T. J., Schröder, C., et al. (2011). Evidence for mechanical and chemical alteration of iron-nickel meteorites on Mars: Process insights for Meridiani Planum. *Journal of Geophysical Research*, 116, E00F20. <https://doi.org/10.1029/2010JE003672>
- Bagnold, R. A. (1941). *The physics of blown sand and desert dunes*. New York, Methuen: Dover Publications Inc.
- Balme, M., & Hagermann, A. (2006). Particle lifting at the soil-air interface by atmospheric pressure excursions in dust devils. *Geophysical Research Letters*, 33, L19S01. <https://doi.org/10.1029/2006GL026819>
- Bevan, A. W. R., Bland, P. A., & Jull, A. J. T. (1998). Meteorite flux on the Nullarbor Region, Australia. *Geological Society London Special Publications*, 140(1), 59–73. <https://doi.org/10.1144/GSL.SP.1998.140.01.07>
- Bish, D. L., Blake, D. F., Vaniman, D. T., Chipera, S. J., Morris, R. V., Ming, D. W., et al. (2013). X-ray diffraction results from Mars Science Laboratory: Mineralogy of Rocknest at Gale Crater. *Science*, 341(6153), 1238932. <https://doi.org/10.1126/science.1238932>
- Bland, P., & Smith, T. B. (2000). Meteorite accumulations on Mars. *Icarus*, 144(1), 21–26. <https://doi.org/10.1006/icar.1999.6253>
- Borin, P., Cremonese, G., Marzari, F., & Lucchetti, A. (2017). Asteroidal and cometary dust flux in the inner solar system. *Astronomy & Astrophysics*, 605, A94. <https://doi.org/10.1051/0004-6361/201730617>
- Brimblecombe, P. (2014). The global sulfur cycle. In D. M. Karl & W. H. Schlesinger (Eds.), *Treatise in Geochemistry* (p. 9144), Vol. 10, *Biogeochemistry* (Chapter 10.14, pp. 559–591). Elsevier Science. <https://doi.org/10.1016/B978-0-08-095975-7.00814-7>
- Brinton, K. L. F., Engrand, C., Glavin, D. P., Bada, J. L., & Maurette, M. (1998). A search for extraterrestrial amino acids in carbonaceous Antarctic micrometeorites. *Origins of Life and Evolution of Biospheres*, 28(4/6), 413–424. <https://doi.org/10.1023/A:1006548905523>
- Carr, M. H., & Head, J. W. (2010). Geologic history of Mars. *Earth and Planetary Science Letters*, 294(3-4), 185–203. <https://doi.org/10.1016/j.epsl.2009.06.042>
- Carr, M. H., & Head, J. W. (2015). Martian surface/near-surface water inventory: Sources, sinks, and changes with time. *Geophysical Research Letters*, 42, 726–732. <https://doi.org/10.1002/2014GL024644>
- Carrillo-Sánchez, J. D., Nesvorný, D., Pokorný, P., Janches, D., & Plane, J. M. C. (2016). Sources of cosmic dust in the Earth's atmosphere. *Geophysical Research Letters*, 43, 11,979–11,986. <https://doi.org/10.1002/2016GL071697>
- Carrillo-Sánchez, J. D., Plane, J. M. C., Feng, W., Nesvorný, D., & Janches, D. (2015). On the size and velocity distribution of cosmic dust particle entering the atmosphere. *Geophysical Research Letters*, 42, 6518–6525. <https://doi.org/10.1002/2015GL065149>
- Catling, D. C., & Kasting, J. F. (2017). *Atmospheric evolution on inhabited and lifeless worlds*. Cambridge, United Kingdom: Cambridge University Press. <https://doi.org/10.1017/9781139020558>
- Chaffin, M. S., Deighan, J., Schneider, N. M., & Stewart, A. I. F. (2017). Elevated atmospheric escape of atomic hydrogen from Mars induced by high-altitude water. *Nature Geoscience*, 10(3), 174–178. <https://doi.org/10.1038/ngeo2887>
- Cordier, C., & Folco, L. (2014). Oxygen isotopes in cosmic spherules and the composition of the near Earth interplanetary dust complex. *Geochimica et Cosmochimica Acta*, 146, 18–26. <https://doi.org/10.1016/j.gca.2014.09.038>
- Dartois, E., Engrand, C., Brunetto, R., Duprat, J., & Icarus, T. P. (2013). Ultracarbonaceous Antarctic micrometeorites, probing the solar system beyond the nitrogen snow-line. *Icarus*, 224(1), 243–252. <https://doi.org/10.1016/j.icarus.2013.03.002>
- Dodd, R. T. (1976). Accretion of the ordinary chondrites. *Earth and Planetary Science Letters*, 30(2), 281–291. [https://doi.org/10.1016/0012-821X\(76\)90255-7](https://doi.org/10.1016/0012-821X(76)90255-7)
- Duprat, J., Dobrica, E., Engrand, C., Aléon, J., Marrocchi, Y., Mostefaoui, S., et al. (2010). Extreme deuterium excesses in ultracarbonaceous micrometeorites from central Antarctic snow. *Science*, 328(5979), 742–745. <https://doi.org/10.1126/science.1184832>

- Duprat, J., Engrand, C., Maurette, M., Kurat, G., Gounelle, M., & Hammer, C. (2007). Micrometeorites from Central Antarctic snow: The CONCORDIA collection. *Advances in Space Research*, 39(4), 605–611. <https://doi.org/10.1016/j.asr.2006.05.029>
- Farley, K. A., Malespin, C., Mahaffy, P., Grotzinger, J. P., Vasconcelos, P. M., Milliken, R. E., et al. (2014). In situ radiometric and exposure age dating of the Martian surface. *Science*, 343(6169). <https://doi.org/10.1126/science.1247166>
- Flynn, G. J., & McKay, D. S. (1990). An assessment of the meteoritic contribution to martian soil. *Journal of Geophysical Research*, 95(B9), 14,497–14,509. <https://doi.org/10.1029/JB095iB09p14497>
- Folco, L., & Cordier, C. (2015). Micrometeorites. In M. R. Lee & H. Leroux (Eds.), *EMU Notes in Mineralogy, The European Mineralogical Union and the Mineralogical Society of Great Britain & Ireland* (pp. 253–297).
- Forget, F., Haberle, R. M., Montmessin, F., Levrard, B., & Head, J. W. (2006). Formation of glaciers on Mars by atmospheric precipitation at high obliquity. *Science*, 311(5759), 368–371. <https://doi.org/10.1126/science.1120335>
- Genge, M. (2016). The origins of I-type spherules and the atmospheric entry of iron micrometeoroids. *Meteoritics & Planetary Science*, 51(6), 1063–1081. <https://doi.org/10.1111/maps.12645>
- Genge, M., Engrand, C., Gounelle, M., & Taylor, S. (2008). The classification of micrometeorites. *Meteoritics & Planetary Science*, 43(3), 497–515. <https://doi.org/10.1111/j.1945-5100.2008.tb00668.x>
- Genge, M. J., Davies, B., Suttle, M. D., van Ginneken, M., & Tomkins, A. G. (2017). The mineralogy and petrology of I-type cosmic spherules: Implications for their sources, origins and identification in sedimentary rocks. *Geochimica et Cosmochimica Acta*, 218, 167–200. <https://doi.org/10.1016/j.gca.2017.09.004>
- Grun, E., Zook, H. A., Fechtig, H., & Giese, R. H. (1985). Collisional balance of the meteoritic complex. *Icarus*, 62(2), 244–272. [https://doi.org/10.1016/0019-1035\(85\)90121-6](https://doi.org/10.1016/0019-1035(85)90121-6)
- Gull, M., Mojica, M. A., Fernández, F. M., Gaul, D. A., Orlando, T. M., Liotta, C. L., & Pasek, M. A. (2015). Nucleoside phosphorylation by the mineral schreibersite. *Science Report*, 5(1), 17198. <https://doi.org/10.1038/srep17198>
- Hartmann, W. K. (2005). Martian cratering 8: Isochron refinement and the chronology of Mars. *Icarus*, 174(2), 294–320. <https://doi.org/10.1016/j.icarus.2004.11.023>
- Hynek, B. (2016). The great climate paradox of ancient Mars. *Geology*, 44(10), 879–880. <https://doi.org/10.1130/focus102016.1>
- Hynek, B., & Phillips, R. J. (2008). The stratigraphy of Meridiani Planum, Mars, and implications for the layered deposits' origin. *Earth and Planetary Science Letters*, 274(1–2), 214–220. <https://doi.org/10.1016/j.epsl.2008.07.025>
- Jackson, D. W. T., Bourke, M. C., & Smyth, T. A. G. (2015). The dune effect on sand-transporting winds on Mars. *Nature Communications*, 6(1), 8796. <https://doi.org/10.1038/ncomms9796>
- Jakosky, B. M., Slipski, M., Benna, M., Mahaffy, P., Elrod, M., Yelle, R., et al. (2017). Mars' atmospheric history derived from upper-atmosphere measurements of <sup>38</sup>Ar/<sup>36</sup>Ar. *Science*, 355(6332), 1408–1410. <https://doi.org/10.1126/science.aai7721>
- Khisina, N. R., Badyukov, D. D., & Wirth, R. (2016). Microtexture, nanomineralogy, and local chemistry of cryptocrystalline cosmic spherules. *Geochemistry International*, 54(1), 68–77. <https://doi.org/10.1134/S0016702916010067>
- Kirkby, C. A., Kirkegaard, J. A., Richardson, A. E., Wade, L. J., Blanchard, C., & Batten, G. (2011). Stable soil organic matter: A comparison of C:N:P:S ratios in Australian and other world soils. *Geoderma*, 163(3–4), 197–208. <https://doi.org/10.1016/j.geoderma.2011.04.010>
- Li, Y., Ratchev, I. P., Lucas, J. A., Evans, G. M., & Belton, G. R. (2000). Rate of interfacial reaction between liquid iron oxide and CO-CO<sub>2</sub>. *Metallurgical and Materials Transactions B*, 31(5), 1049–1057. <https://doi.org/10.1007/s11663-000-0080-5>
- Love, S. G., & Brownlee, D. E. (1991). Heating and thermal transformation of micrometeoroids entering the Earth's atmosphere. *Icarus*, 89(1), 26–43. [https://doi.org/10.1016/0019-1035\(91\)90085-8](https://doi.org/10.1016/0019-1035(91)90085-8)
- Love, S. G., & Brownlee, D. E. (1993). A direct measurement of the terrestrial mass accretion rate. *Science*, 262, 550–553.
- Lybrand, R. A., Michalski, G., Graham, R. C., & Parker, D. R. (2013). The geochemical associations of nitrate and naturally formed perchlorate in the Mojave desert, California, USA. *Geochimica et Cosmochimica Acta*, 104, 136–147. <https://doi.org/10.1016/j.gca.2012.10.028>
- Mangold, N., Ansan, V., Masson, P., & Vincendon, C. (2009). Estimate of aeolian dust thickness in Arabia Terra, Mars: Implications of a thick mantle (>20 m) for hydrogen detection. *Geomorphic*, 15(1), 23–32. <https://doi.org/10.4000/geomorphologie.7472>
- Mitra, K., and J. G. Catalano (2017). Iron oxidation by chlorate: Implications for akaganéite and jarosite formation on Mars, in Fourth International Conference on Early Mars: Geologic, Hydrologic, and Climatic Evolution and the Implications for Life, edited, pp. LPI Contribution No. 2014, 2017, id.3008, Flagstaff, Arizona.
- Morgan, T. H., Zook, J. A., & Potter, A. E. (1988). Impact-driven supply of sodium and potassium to the atmosphere of Mercury. *Icarus*, 75(1), 156–170. [https://doi.org/10.1016/0019-1035\(88\)90134-0](https://doi.org/10.1016/0019-1035(88)90134-0)
- Morowitz, H. J. (1968). *Energy flow in biology: Biological organization as a problem in thermal physics*. New York: Academic Press.
- Nisbet, E. G., & Fowler, C. M. R. (2014). The early history of life. In D. M. Karl, & W. H. Schlesinger (Eds.), *Treatise in Geochemistry* (p. 9144), Vol. 10, *Biogeochemistry* (Chapter 10.1, pp. 1–42). Elsevier Science. <https://doi.org/10.1016/B978-0-08-095975-7.00801-9>
- Onoue, T., Nakamura, T., Haranosono, T., & Yasuda, C. (2011). Composition and accretion rate of fossil micrometeorites recovered in Middle Triassic deep-sea deposits. *Geology*, 39(6), 567–570. <https://doi.org/10.1130/G31866.1>
- Orosei, R., Lauro, S. E., Pettinelli, E., Cicchetti, A., Coradini, M., Cosciotti, B., et al. (2018). Radar evidence of subglacial liquid water on Mars. *Science*, 361(6401), 490–493. <https://doi.org/10.1126/science.aar7268>
- Owen, T., Biemann, D. R., Rushneck, J. E., Biller, J. E., Howarth, D. W., & Lafleui, A. L. (1977). The composition of the atmosphere at the surface of Mars. *Journal of Geophysical Research*, 82(28), 4635–4639. <https://doi.org/10.1029/JS082i028p04635>
- Pack, A., Howeling, A., Hezel, D. C., Stefanak, M. T., Beck, A.-K., Peters, S. T. M., et al. (2017). Tracing the oxygen isotope composition of the upper Earth's atmosphere using cosmic spherules. *Nature Communications*, 8(1), 15,702. <https://doi.org/10.1038/ncomms15702>
- Pasek, M., Herschy, B., & Kee, T. P. (2015). Phosphorus: A case for mineral-organic reactions in prebiotic chemistry. *Origins Life Evolution Biospheres*, 45(1–2), 207–218. <https://doi.org/10.1007/s11084-015-9420-y>
- Pasek, M., & Lauretta, D. S. (2008). Extraterrestrial flux of potentially prebiotic C, N, and P to the early Earth. *Origins Life Evolution Biospheres*, 38(1), 5–21. <https://doi.org/10.1007/s11084-007-9110-5>
- Quantin-Nataf, C., Craddock, R. A., Dubuffet, F., Lozac'h, L., & Martinot, M. (2019). Decline of crater obliteration rates during early Martian history. *Icarus*, 317, 427–433. <https://doi.org/10.1016/j.icarus.2018.08.005>
- Radzilowski, R. H., & Pehlke, R. D. (1978). Absorption of gaseous oxygen by liquid cobalt, copper, iron and nickel. *Metallurgical and Materials Transactions*, 9(1), 129–137. <https://doi.org/10.1007/BF02822680>
- Rimmer, P. B., Shorttle, O., & Rugheimer, S. (2019). Oxidised micrometeorites as evidence for low atmospheric pressure on the early Earth. *Geochimica et Cosmochimica Acta*, 253, 38–42.
- Rochette, P., Folco, L., Suavet, C., van Ginneken, M., Gattacceca, J., Perchiazzi, N., et al. (2008). Micrometeorites from the Transantarctic Mountains. *Proceedings of the National Academy of Sciences*, 105, 18,206–18,211.



- Schröder, C., Bland, P. A., Golombek, M. P., Ashley, J. W., Warner, N. H., & Grant, J. A. (2016). Amazonian chemical weathering rate derived from stony meteorite finds at Meridiani Planum on Mars. *Nature Communications*, 7(1), 13459. <https://doi.org/10.1038/ncomms13459>
- Schroder, C., Bland, P. A., Golombek, M. P., Ashley, J. W., Warner, N. H., & Grant, J. A. (2016). Amazonian chemical weathering rate derived from stony meteorite finds at Meridiani Planum on Mars. *Nature Communications*, 7(1), 13459. <https://doi.org/10.1038/ncomms13459>
- Schröder, C., Rodionov, D. S., McCoy, T. J., Jolliff, B. L., Gellert, R., Nittler, L. R., et al. (2008). Meteorites on Mars observed with the Mars Exploration Rovers. *Journal of Geophysical Research*, 113, E06S22. <https://doi.org/10.1029/2007JE002990>
- Southworth, S. A., and Z. Sekanina (1973), Physical and dynamical studies of meteors. NASA Conference Report, edited, pp. CR-2316.
- Stein, N., Grotzinger, J. P., Schieber, J., Mangold, N., Hallet, B., Newsom, H., et al. (2018). Desiccation cracks provide evidence of lake drying on Mars, Sutton Island member, Murray Formation, Gale Crater. *Geology*, 46(6), 515–518. <https://doi.org/10.1130/G40005.1>
- Stern, J. C., Sutter, B., Freissinet, C., Navarro-González, R., McKay, C. P., Archer, P. D. Jr., et al., & the MSL Science Team (2015). Evidence for indigenous nitrogen in sedimentary and aeolian deposits from the Curiosity rover investigations at Gale Crater, Mars. *Proceedings of the National Academy of Sciences*, 112(14), 4245–4250. <https://doi.org/10.1073/pnas.1420932112>
- Stern, J. C., Sutter, B., Jackson, W. A., Navarro-González, R., McKay, C. P., Ming, D. W., et al. (2017). The nitrate/(per) chlorate relationship on Mars. *Geophysical Research Letters*, 44, 2643–2651. <https://doi.org/10.1002/2016GL072199>
- Suttle, M. D., & Genge, M. (2017). Diagenetically altered fossil micrometeorites suggest cosmic dust is common the geological record. *Earth and Planetary Science Letters*, 476, 132–142. <https://doi.org/10.1016/j.epsl.2017.07.052>
- Tachibana, S., & Tsuchiyama, A. (1998). Incongruent evaporation of troilite (FeS) in the primordial solar nebula: An experimental study. *Geochimica et Cosmochimica Acta*, 62(11), 2005–2022. [https://doi.org/10.1016/S0016-7037\(98\)00122-7](https://doi.org/10.1016/S0016-7037(98)00122-7)
- Tait, A. W., Gagen, E. J., Wilson, S. A., Tomkins, A. G., & Southam, G. (2017). Microbial populations of stony meteorites: Substrate controls on first colonisers. *Frontiers in Microbiology*, 8.
- Tait, A. W., Wilson, S. A., Tomkins, A. G., Gagen, E. J., Fallon, S. J., & Southam, G. (2017). Evaluation of meteorites as habitats for terrestrial microorganisms: Results from the Nullarbor Plain, Australia, a Mars analogue site. *Geochimica et Cosmochimica Acta*, 215, 1–16. <https://doi.org/10.1016/j.gca.2017.07.025>
- Tanaka, K. L., & Hartmann, W. K. (2012). The planetary time scale. In F. M. Gradstein, J. G. Ogg, M. D. Schmitz & G. M. Ogg (Eds.), *The geologic time scale* (Chapter 15, p. 275–298). Elsevier. 1176 p. <https://doi.org/10.1016/B978-0-444-59425-9.00015-9>
- Taylor, S., Lever, J. H., & Harvey, R. P. (1998). Accretion rate of cosmic spherules measured at South Pole. *Science*, 392, 899–903.
- Taylor, S., Lever, J. H., & Harvey, R. P. (2000). Numbers, types, and compositions of an unbiased collection of cosmic spherules. *Meteoritics & Planetary Science*, 35(4), 651–666. <https://doi.org/10.1111/j.1945-5100.2000.tb01450.x>
- Tomkins, A. G., Bowlt, L., Genge, M., Wilson, S. A., Brand, H. E. A., & Wykes, J. L. (2016). Ancient micrometeorites suggestive of an oxygen-rich Archean upper atmosphere. *Nature*, 533(7602), 235–238. <https://doi.org/10.1038/nature17678>
- Viksman, G. S., & Gordienko, S. P. (1992). Behavior in vacuum at high temperatures and thermodynamic properties of nickel phosphide Ni<sub>3</sub>P. *Powder Metallurgy Metal Ceramics*, 31(12), 1052–1053. <https://doi.org/10.1007/BF00797769>
- Weiss, M. C., Sousa, F. L., Mrnjavac, N., Neukirchen, S., Roettger, M., Nelson-Sathi, S., & Martin, W. F. (2016). The physiology and habitat of the last universal common ancestor. *Nature Microbiology*, 1(9), 16116. <https://doi.org/10.1038/nmicrobiol.2016.116>
- Wordsworth, R. D. (2016). The climate of early Mars. *Annual Review of Earth and Planetary Sciences*, 44, 1–31.
- Yen, A. S., Mittlefehldt, D. W., McLennan, S. M., Gellert, R., Bell, J. F. III, McSween, H. Y. Jr., et al. (2006). Nickel on Mars: Constraints on meteoritic material at the surface. *Journal of Geophysical Research*, 111(E12), E12S11. <https://doi.org/10.1029/2006JE002797>